

Fabrication and characterization of all-Nb lumped-element Josephson parametric amplifiers

Hang Xue(薛航), Zhirong Lin(林志荣), Wenbing Jiang(江文兵), Zhengqi Niu(牛铮琦), Kuang Liu(刘匡), Wei Peng(彭炜), and Zhen Wang(王镇)

Citation: Chin. Phys. B, 2021, 30 (**6**): 068503. DOI: 10.1088/1674-1056/abeee6
Journal homepage: http://cpb.iphy.ac.cn; http://iopscience.iop.org/cpb

What follows is a list of articles you may be interested in

An easily-prepared impedance matched Josephson parametric amplifier

Ya-Peng Lu(卢亚鹏), Quan Zuo(左权), Jia-Zheng Pan(潘佳政), Jun-Liang Jiang(江俊良), Xing-Yu Wei(魏兴雨), Zi-Shuo Li(李子硕), Wen-Qu Xu(许问渠), Kai-Xuan Zhang(张凯旋), Ting-Ting Guo(郭婷婷), Shuo Wang(王硕), Chun-Hai Cao(曹春海), Wei-Wei Xu(许伟伟), Guo-Zhu Sun(孙国柱), and Pei-Heng Wu(吴培亨)

Chin. Phys. B, 2021, 30 (**6**): 068504. DOI: 10.1088/1674-1056/ac0420

Controllable microwave frequency comb generation in a tunable superconducting coplanar-waveguide resonator

Shuai-Peng Wang(王帅鹏), Zhen Chen(陈臻), and Tiefu Li(李铁夫)

Chin. Phys. B, 2021, 30 (**4**): 048501. DOI: 10.1088/1674-1056/abc2bb

Manipulation of superconducting qubit with direct digital synthesis

Zhi-Yuan Li(李志远), Hai-Feng Yu(于海峰), Xin-Sheng Tan(谭新生), Shi-Ping Zhao(赵士平), Yang Yu(于扬)

Chin. Phys. B, 2019, 28 (**9**): 098505. DOI: 10.1088/1674-1056/ab37f9

Development of 0.5-V Josephson junction array devices for quantum voltage standards

Lanruo Wang(王兰若), Jinjin Li(李劲劲), Wenhui Cao(曹文会), Yuan Zhong(钟源), Zhonghua Zhang(张钟华)

Chin. Phys. B, 2019, 28 (**6**): 068501. DOI: 10.1088/1674-1056/28/6/068501

Characterization of barrier-tunable radio-frequency-SQUID for Maxwell's demon experiment

Gang Li(李刚), Suman Dhamala, Hao Li(李浩), Jian-She Liu(刘建设), Wei Chen(陈炜)

Chin. Phys. B, 2018, 27 (**6**): 068501. DOI: 10.1088/1674-1056/27/6/068501

SPECIAL TOPIC — Quantum computation and quantum simulation

Fabrication and characterization of all-Nb lumped-element Josephson parametric amplifiers*

Hang Xue(薛航)[1,2,3], Zhirong Lin(林志荣)[1,2,3,†], Wenbing Jiang(江文兵)[1,3], Zhengqi Niu(牛铮琦)[1,2,3,4], Kuang Liu(刘匡)[1,2,3], Wei Peng(彭炜)[1,2,3], and Zhen Wang(王镇)[1,2,3,4]

[1] *State Key Laboratory of Functional Materials for Informatics, Shanghai Institute of Microsystem and Information Technology (SIMIT), Chinese Academy of Sciences, Shanghai* 200050, *China*

[2] *University of Chinese Academy of Sciences, Beijing* 100049, *China*

[3] *CAS Center for Excellence in Superconducting Electronics (CENSE), Shanghai* 200050, *China*

[4] *ShanghaiTech University, Shanghai* 201210, *China*

(Received 13 January 2021; revised manuscript received 25 February 2021; accepted manuscript online 16 March 2021)

Josephson parametric amplifiers (JPAs) with nearly quantum-limited noise performance have become indispensable devices for the measurements of superconducting quantum information. We have developed an all-Nb lumped-element flux-driven JPA operating in the three-wave mixing mode. Our Nb-based JPA comprises Nb/Al-AlO$_x$/Nb Josephson junctions, a parallel-plate capacitor with SiO_2 dielectric sandwiched between two Nb layers, a bottom coplanar waveguides layer, and a top Nb wiring layer. We experimentally demonstrate a 20 dB gain over a 190 MHz bandwidth, a mean 1 dB compression of −123 dBm, and near quantum-limited noise performance. This fabrication process can be further used to design impedance transformed parametric amplifiers for multiple-qubit readout.

Keywords: Josephson parametric amplifier, Nb/Al-AlO$_x$/Nb Josephson junctions, lumped-element resonator

PACS: 85.25.Cp, 85.25.Am, 85.25.Dq **DOI:** 10.1088/1674-1056/abeee6

1. Introduction

Superconducting parametric amplifiers based on Josephson junctions have been widely used in the past decade because of their capabilities to provide amplification with a noise performance near the quantum limit.[1–5] The unique characteristics of Josephson parametric amplifiers enable them to be applied to weak measurement,[6] quantum feedback,[7] squeezed microwave[8] and qubit readout.[9–11] In previous works, two kinds of parametric amplifiers have been developed, one based on individual resonant architecture[12–15] and the other named Josephson traveling wave parametric amplifier (JTWPA) based on Josephson junction transmission line.[16–18] JTWPA has extraordinary bandwidth and saturation power, however its fabrication process is complicated and requires thousands of Josephson junction units. On the other hand, the impedance transformed parametric amplifier (IMPA) based on lumped-element Josephson parametric amplifier (LJPA)[4] has the best performance among resonant-type JPA. LJPA includes much fewer Josephson junctions in the dc superconducting quantum interference device (SQUID), and supplies the profits of broad bandwidth of several hundred MHz and near quantum-limited performance.[19–21] The Josephson junctions were fabricated using standard Al/AlO$_x$/Al tunnel junction with shadow evaporation.[22,23] Sandwich structures of parallel-plate capacitors in LJPA were fabricated independently of junctions.[19,20] The uniformity of the lumped-element LC resonators comprised of parallel-plate capacitors and Al Josephson junctions makes it challenging to prepare Al junction-based JTWPA device that requires thousands of units.

In addition, Nb-based multilayer process is compatible with the existing commercial semiconductor micro-fabrication platforms. All-refractory Nb/Al-AlO$_x$/Nb Josephson junctions are robust after several thermal cycles. The fabrication technology of Nb/Al-AlO$_x$/Nb junctions is currently well-established and is usually used for the fabrication of superconducting devices such as single-flux-quantum (SFQ) logic circuits, programmable Josephson voltage standards, and dc SQUIDs.[24–26] Recently, the reliable and reproducible fabrication process for high quality Nb/Al-AlO$_x$/Nb junctions with small leakage currents was developed.[27] The high uniformity of the properties of the Nb-based junctions has the potential to develop JTWPA.

In this paper, we report the fabrication and characterization of LJPAs using a multilayer micro-fabrication process.[28] The LJPAs are comprised of Nb/Al-AlO$_x$/Nb junctions and Nb/SiO_2/Nb parallel-plate capacitors. The fabrication process is based on dry etching of the Nb/Al-AlO$_x$/Nb trilayer

*Project supported by the National Natural Science Foundation of China (Grant No. 92065116), Strategic Priority Research Program of the Chinese Academy of Sciences (Grant No. XDA18000000), and the Key-Area Research and Development Program of Guangdong Province, China (Grant No. 2020B0303030002).

†Corresponding author. E-mail: zrlin@mail.sim.ac.cn

© 2021 Chinese Physical Society and IOP Publishing Ltd

on intrinsic silicon. In Nb trilayer junction process, we typically make a SiO_2 layer as an electrical isolation layer and a wiring Nb layer on top of the SiO_2 layer to connect part of top and bottom Nb layers. The parallel-plate capacitors are fabricated at the same time owing to the overlapped layers of the wiring Nb layer, the bottom Nb layer, and the intermediate SiO_2 layer. We experimentally demonstrated 190 MHz of almost 3 dB smooth bandwidth with a 20 dB gain centered around 6.848 GHz. Within the entire bandwidth of the amplifier, an average 1 dB compression point of −123 dBm with the near-quantum-limited noise performance makes it have the potential to be applied in broadband IMPA and multi-qubit readout.

2. Design and device fabrication

The design of the LJPAs we fabricated is similar to the ones reported by Mutus *et al.*[19] As shown in the schematic circuit and optical micrograph in Figs. 1(a) and 1(b), the oscillating system includes of a SQUID with flux-dependence nonlinear inductance shunted by a parallel plate capacitor. The parametric amplifier resonator whose resonant frequency can be tuned in the 4–8 GHz range by adjusting the static magnetic flux threading the SQUID loop is directly coupled to a single input–output signal line. An on-chip pump line, which is realized by a 50 Ω transmission line, provides an ac flux and energy of parametric amplification.[29] These amplifiers have an unbiased nonlinear junction inductance $L_J = 54.9$ pH, a geometric inductance $L_g = 13.39$ pH, a capacitance of $C = 5.68$ pF, producing a resonant frequency $f_0 = 1/2\pi((L_J + L_g)C)^{1/2} = 8.08$ GHz. The coupled quality factor (Q) of the LJPA is expressed as $Q = 2\pi Z f_0 C = 14.4$, where Z is 50 Ω of the environmental impedance.[19]

The LJPAs based on Nb/Al–AlO_x/Nb Josephson tunnel junctions were fabricated with multilayer processes in the Superconducting Electronics Facility (SELF) at Shanghai Institute of Microsystem and Information Technology. In the first step, Nb/Al–AlO_x/Nb trilayer was deposited on an intrinsic silicon substrate *in-situ* in a combination equipment with separate chambers for dc magnetron sputtering of Nb, Al, and for AlO_x formation by static oxidation. Nb base and counter electrodes were both 150 nm-thick and the Al film was 10 nm-thick. The thickness of the AlO_x barrier which determines the critical current density of the Josephson junction can be controlled with the oxygen exposure. Appropriate oxygen pressure and exposure time for oxidation were adjusted to obtain the Josephson critical current density of about 100 A/cm^2. In the second step, a layer of photoresist AZ703 was spin-coated above HMDS and baked. We used a Canon FPA-3030 i5+ stepper with 350 nm imaging resolution for photolithography of all layers. The Nb/Al-AlO_x/Nb Josephson junctions we used were designed as circular-shaped and defined by etching the top Nb layer. After that, lithography and wet etching were performed to define the AlO_x barrier whose area must be larger than junction's so that the barrier between the Nb base and counter electrode was not damaged during the process. The Nb layer was etched via a process using inductively coupled plasma (ICP), then the AlO_x barrier was wet etched using developer. In the third step, the transmission line and Nb base electrode were defined by reactive ion etching (RIE) the bottom Nb layer. In the fourth step, a 250 nm-thick SiO_2 film was deposited using a plasma enhanced chemical vapor deposition (PECVD) process and etched using CHF_3 to form an electrical isolation layer between the bottom Nb electrode, the transmission line, and the wiring layer. The dielectric layers used for capacitors and contact holes for vias through the SiO_2 layer were also made. In the fifth step, a 300 nm-thick Nb film was deposited and etched to form the top electrodes of the shunt capacitors and the crossovers on the signal and pump lines. This layer was also used to form the shunt connections between the Josephson junctions and parallel plate capacitors, meanwhile, the electrical connections between the junctions and the ground.

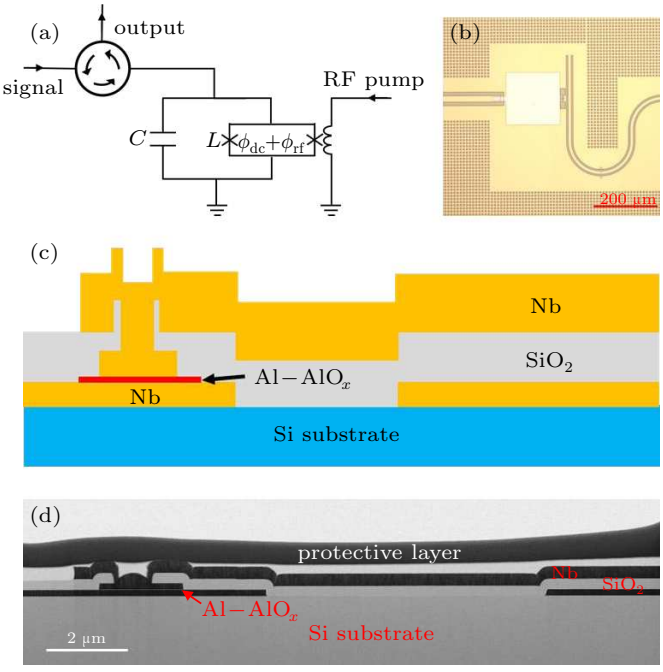


Fig. 1. (a) Circuit diagram of LJPA. The input signal is amplified and reflected from the resonant circuit through a circulator, which is used to separate the input signal and output signal. An external magnetic flux ϕ_{dc} provided by a superconducting coil and an ac magnetic flux ϕ_{rf} supplied by pump line tunes the resonant frequency. (b) The optical micrograph of the device. The center square indicates the parallel plate capacitor. The 50 Ω coplanar waveguides in the left and right indicate the signal and pump lines, respectively. (c) Schematic of the cross-section of LJPA. A structure of 10 nm thick Al–AlO_x sandwiched between two Nb layers forms a Josephson junction. A wiring layer on the top is isolated from the bottom Nb by a silicon oxide, and a parallel plate capacitor is formed as shown in the right side of the graph. The schematic diagram is not displayed to scale. (d) Cross-sectional TEM micrograph of our LJPA as shown in (c). The top layer is the protective layer used in TEM sample preparation.

Figures 1(c) and 1(d) show a schematic of cross-section and the corresponding transmission electron microscopy (TEM) micrograph of a Nb-based junction and a part of parallel plate capacitor on a silicon substrate. These integrated LC resonators were mass fabricated using wafer-scale process, which produced hundreds of devices at the same time and could be further used to make IMPA and JTWPA.

3. Measurements and results

In LJPA characterization measurements, the sample is anchored to the sample stage of a dilution refrigerator with a base temperature around 17 mK. This paper includes two devices, labeled A and B, whose designs are identical. They were simultaneously fabricated on one substrate. Before operating the device as a parametric amplifier, we first characterized the resonator's reflectance with a signal tone. A superconducting coil is used to supply the dc flux bias and tune the resonant frequency of LJPA by adjusting the magnetic flux penetrating the SQUID loop. Figures 2(a) and 2(b) show the resonant frequency as a function of the flux bias for the LJPA we made. The solid red line is the theoretical prediction from the designed parameters. Resonant frequency of the LJPA can be tuned from 4 GHz to 8 GHz by adjusting the bias current in the superconducting coil. The modulation curve of device A is experimentally discontinuous, but the period of flux modulation can still be observed. This phenomenon also exists in other devices fabricated at the same time. We apply the magnetic field with the external coils in the sample holder. The phenomenon we observed is that the frequency is kindly "latched" when we change the dc current in small range of the external coils. Then it jumps to next frequency suddenly. We speculate that it is due to magnetic flux crosstalk caused by a larger loop where the SQUID loop is included. Also, this phenomenon may be caused by poor contacts between crossovers and the bottom Nb layers which are due to the inhomogeneity of etching of SiO_2 in the fabrication process. Poor contact leads to unequal grounding on two sides of the central conductor, resulting in parasitic modes. Furthermore, there is no grounding meshes near the SQUID. The flux trapping may also cause discontinuities. In subsequent design, we try to improve the magnetic flux jump by increasing the area of the loops around SQUIDs and placing proper crossovers. By fitting theoretical formula to the experimental modulation curve of the LJPA, the zero-field Josephson critical current I_c and shunt capacitance can be obtained. The extracted I_c is about 3 μA which is close to the I–V curve measurement result at 4.2 K. The extracted C is about 5.78 pF, which is close to the design value. The quality factor obtained by fitting S_{21} curve under zero flux bias is approximately equal to 11, which is close to the design value.

The LJPA we fabricated can be operated in either a three-wave mixing mode or a four-wave mixing mode. We characterized our devices as a three-wave mixing amplifier by driving RF flux via the SQUID loop with the inductively coupled pump line.[4] The appropriate pump frequency and pump power are optimized to realize large gain at different dc flux biases. The data in Figs. 3(a) and 3(b) display bandwidths of devices A and B with a 20 dB gain at three flux biases. In device A, a gain of 20 dB in the bandwidth of 190 MHz (centered around 6.848 GHz) was observed, as shown in Fig. 3(a). The pump frequency is around 13.696 GHz. The pump power is around −25.8 dBm at the pump port. The flux bias is around $0.276\phi_0$, where ϕ_0 is the flux quantum. The large bandwidth in the LJPA is expected to be further improved by engineering the impedance transformer.

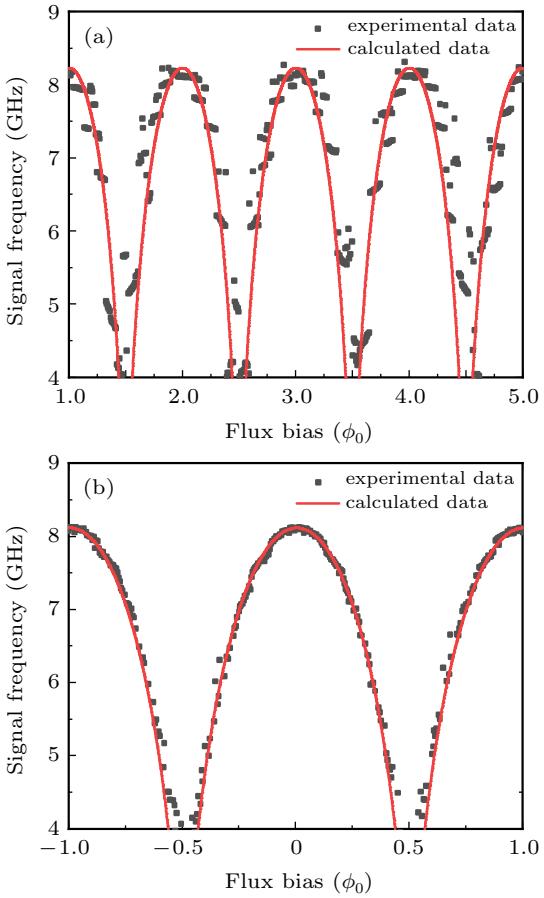


Fig. 2. DC flux modulation. Experimental data of resonant frequency vs. flux bias is plotted by fitting the measured phase of the reflected microwave. The theoretical line is plotted by fitting the experimental data. (a) Modulation curve of device A. The modulation curve is discontinuous, but the resonant frequency of the LJPA can still be tuned from 4 GHz to 8 GHz. (b) Modulation curve of device B. The resonant frequency of device B changes continuously when adjusting the flux bias. The calculated line fits well with the experimental data. The extracted critical current of the Josephson junction is about 3 μA, the extracted capacitance of the parallel-plate capacitor is about 5.78 pF, and the quality factor measured by fitting S_{21} curve under zero flux bias is about 11. These data are close to the designed values.

At each working point, we also measured the saturation power and noise temperature of our LJPA. When the signal

power is high enough, the gain of the amplifier will decrease under the same pump condition. The saturation power is generally described by 1 dB compression point, which refers to the signal power when the gain decreases by 1 dB. The 1 dB compression power is characterized by recording the change of the nondegenerate signal gain with signal input power for a range of pump power [see Fig. 4(a)].

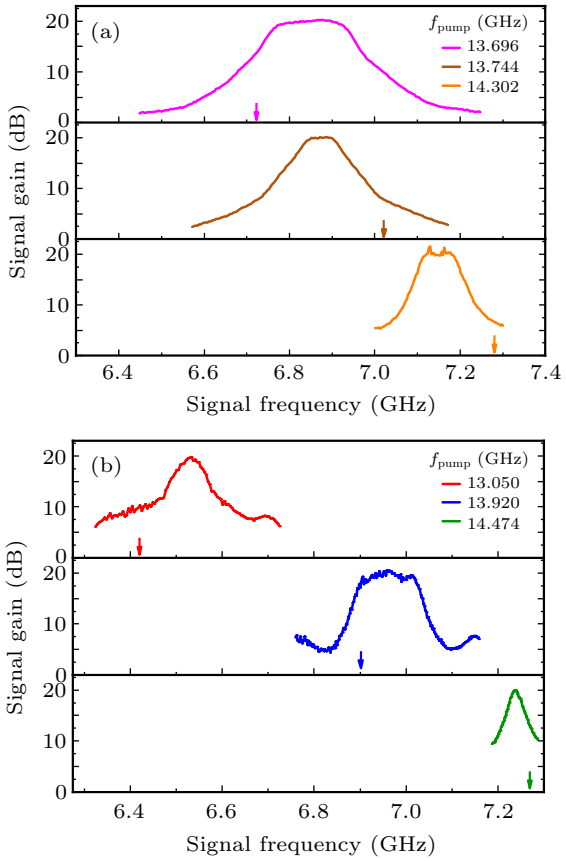


Fig. 3. Signal gain of device A (a) and device B (b) as a function of the signal frequency, for different flux biases and working frequencies. The maximum gain at each working frequency is adjusted to 20 dB. The arrow symbols indicate the positions of the resonant frequency in the absence of parametric pumping.

The noise temperature of LJPA [Fig. 4(b)] was then estimated by comparing the variation of the noise powers when turning on and off the LJPA without the input signal. We have calibrated every amplification and attenuation, such as, HEMT, room temperature amplifier, the circulators, various kinds of filters, and the cable loss between the microwave devices. We infer a lower limit of the noise temperature, around 215.7 mK, from the 9.3 dB increase of the noise power when turning on the LJPA with a 20 dB gain. The noise performance was near quantum-limited, i.e., with a noise temperature of $T_N = hf_R/2k_B \approx 164$ mK, in the full 190 MHz band.[1,30] The bottom panel of Fig. 4(b) shows that the 1 dB compression point has an average value of about −123 dBm for the whole band.

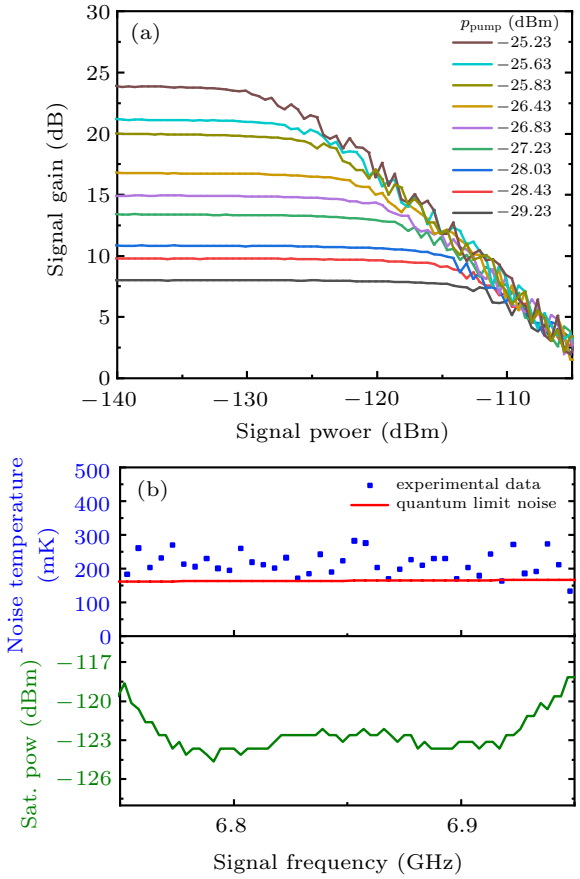


Fig. 4. The saturation power and noise temperature as a function of signal frequency at the working point of Fig. 3(a) with a $0.276\phi_0$ flux bias of device A. (a) Signal gain as a function of the input signal power indicates the saturation at the different pumping powers. (b) The noise temperature of our LJPA and the 1 dB compression point within the 190 MHz bandwidth range.

4. Conclusion and perspectives

In summary, we have designed, fabricated, and characterized the LJPA based on Nb/Al-AlO_x/Nb Josephson tunnel junctions. The fabrication process of Nb-based trilayer junctions we developed yields the parallel-plate capacitors while making the Josephson junctions, which has an ease of use for scalability. We have demonstrated a paramp with a flat gain of 20 dB in the bandwidth of 190 MHz, a saturation power greater than −123 dBm, and near quantum limited noise performance. Our devices fabricated with Nb trilayer process have center frequency tunability and could be used for various superconducting quantum information experiments. In our process, the wiring layers of the devices could be etched and connected with the bottom layers to form crossovers which can be designed to transform the environmental impedance.[19] The process we developed can be further used to fabricate JTWPA that requires thousands of Josephson junctions.

Acknowledgments

The authors would like to thank Liliang Ying, Maezawa Masaaki and all staff at the SELF for the help during the fabrications. The authors appreciate the Chinese medical staff for

keeping us away from COVID-19 to write this paper.

References

[1] Caves C M 1982 *Phys. Rev. D* **26** 1817

[2] Siddiqi I, Vijay R, Pierre F, Wilson C M, Metcalfe M, Rigetti C, Frunzio L and Devoret M H 2004 *Phys. Rev. Lett.* **93** 207002

[3] Reed M D, DiCarlo L, Johnson B R, Sun L, Schuster D I, Frunzio L and Schoelkopf R J 2010 *Phys. Rev. Lett.* **105** 173601

[4] Mutus J Y, White T C, Jeffrey E, Sank D, Barends R, Bochmann J, Chen Y, Chen Z, Chiaro B, Dunsworth A, Kelly J, Megrant A, Neill C, O'Malley P J J, Roushan P, Vainsencher A, Wenner J, Siddiqi I, Vijay R, Cleland A N and Martinis J M 2013 *Appl. Phys. Lett.* **103** 122602

[5] Castellanos-Beltran M A, Irwin K D, Hilton G C, Vale L R and Lehnert K W 2008 *Nat. Phys.* **4** 929

[6] Weber S J, Chantasri A, Dressel J, Jordan A N, Murch K W and Siddiqi I 2014 *Nature* **511** 570

[7] Vijay R, Macklin C, Slichter D H, Weber S J, Murch K W, Naik R, Korotkov A N and Siddiqi I 2012 *Nature* **490** 77

[8] Murch K W, Weber S J, Macklin C and Siddiqi I 2013 *Nature* **502** 211

[9] Lin Z R, Inomata K, Oliver W D, Koshino K, Nakamura Y, Tsai J S and Yamamoto T 2013 *Appl. Phys. Lett.* **103** 132602

[10] Vijay R, Slichter D H and Siddiqi I 2011 *Phys. Rev. Lett.* **106** 110502

[11] Abdo B, Sliwa K, Shankar S, Hatridge M, Frunzio L, Schoelkopf R and Devoret M 2014 *Phys. Rev. Lett.* **112** 167701

[12] Yurke B, Corruccini L R, Kaminsky P G, Rupp L W, Smith A D, Silver A H, Simon R W and Whittaker E A 1989 *Phys. Rev. A* **39** 2519

[13] Yamamoto T, Inomata K, Watanabe M, Matsuba K, Miyazaki T, Oliver W D, Nakamura Y and Tsai J S 2008 *Appl. Phys. Lett.* **93** 042510

[14] Zhong L, Menzel E P, Di Candia R, Eder P, Ihmig M, Baust A, Haeberlein M, Hoffmann E, Inomata K, Yamamoto T, Nakamura Y, Solano E, Deppe F, Marx A and Gross R 2013 *New J. Phys.* **15** 125013

[15] Zhou X, Schmitt V, Bertet P, Vion D, Wustmann W, Shumeiko V and Esteve D 2014 *Phys. Rev. B* **89** 214517

[16] White T C, Mutus J Y, Hoi I C, Barends R, Campbell B, Chen Y, Chen Z, Chiaro B, Dunsworth A, Jeffrey E, Kelly J, Megrant A, Neill C, O'Malley P J J, Roushan P, Sank D, Vainsencher A, Wenner J, Chaudhuri S, Gao J and Martinis J M 2015 *Appl. Phys. Lett.* **106** 242601

[17] Macklin C, O'Brien K, Hover D, Schwartz M E, Bolkhovsky V, Zhang X, Oliver W D and Siddiqi I 2015 *Science* **350** 307

[18] Zorin A B 2016 *Phys. Rev. Appl.* **6** 034006

[19] Mutus J Y, White T C, Barends R, Chen Y, Chen Z, Chiaro B, Dunsworth A, Jeffrey E, Kelly J, Megrant A, Neill C, O'Malley P J J, Roushan P, Sank D, Vainsencher A, Wenner J, Sundqvist K M, Cleland A N and Martinis J M 2014 *Appl. Phys. Lett.* **104** 263513

[20] Roy T, Kundu S, Chand M, Vadiraj A M, Ranadive A, Nehra N, Patankar M P, Aumentado J, Clerk A A and Vijay R 2015 *Appl. Phys. Lett.* **107** 262601

[21] Yang R and Deng H 2020 *IEEE Trans. Appl. Supercond.* **30** 1

[22] Wu Y L, Deng H, Yu H F, Xue G M, Tian Y, Li J, Chen Y F, Zhao S P and Zheng D N 2013 *Chin. Phys. B* **22** 060309

[23] Huang K, Guo Q, Song C, Zheng Y, Deng H, Wu Y, Jin Y, Zhu X and Zheng D 2017 *Chin. Phys. B* **26** 094203

[24] Gurvitch M, Washington M A and Huggins H A 1983 *Appl. Phys. Lett.* **42** 472

[25] Tolpygo S K and Amparo D 2010 *Supercond. Sci. Technol.* **23** 034024

[26] Zhang X, Zhang G, Ying L, Xiong W, Han H, Wang Y, Rong L, Xie X and Wang Z 2018 *Physica C* **548** 1

[27] Kempf S, Ferring A, Fleischmann A, Gastaldo L and Enss C 2013 *Supercond. Sci. Technol.* **26** 065012

[28] Tolpygo S K, Bolkhovsky V, Weir T J, Johnson L M, Gouker M A and Oliver W D 2015 *IEEE Trans. Appl. Supercond.* **25** 1

[29] Hatridge M, Vijay R, Slichter D H, Clarke J and Siddiqi I 2011 *Phys. Rev. B* **83** 134501

[30] Clerk A A, Devoret M H, Girvin S M, Marquardt F and Schoelkopf R J 2010 *Rev. Mod. Phys.* **82** 1155